

This article was downloaded by:[EBSCOHost EJS Content Distribution]  
[EBSCOHost EJS Content Distribution]

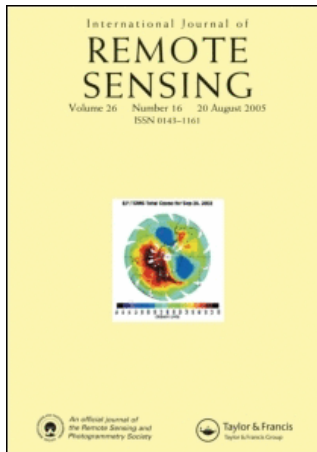
On: 23 July 2007

Access Details: [subscription number 768320842]

Publisher: Taylor & Francis

Informa Ltd Registered in England and Wales Registered Number: 1072954

Registered office: Mortimer House, 37-41 Mortimer Street, London W1T 3JH, UK



## International Journal of Remote Sensing

Publication details, including instructions for authors and subscription information:  
<http://www.informaworld.com/smpp/title~content=t713722504>

### Suitable remote sensing method and data for mapping and measuring active crop fields

Online Publication Date: 01 January 2007

To cite this Article: Xie, H., Tian, Y. Q., Granillo, J. A. and Keller, G. R. , (2007)

'Suitable remote sensing method and data for mapping and measuring active crop fields', International Journal of Remote Sensing, 28:2, 395 - 411

To link to this article: DOI: 10.1080/01431160600702673

URL: <http://dx.doi.org/10.1080/01431160600702673>

PLEASE SCROLL DOWN FOR ARTICLE

Full terms and conditions of use: <http://www.informaworld.com/terms-and-conditions-of-access.pdf>

This article maybe used for research, teaching and private study purposes. Any substantial or systematic reproduction, re-distribution, re-selling, loan or sub-licensing, systematic supply or distribution in any form to anyone is expressly forbidden.

The publisher does not give any warranty express or implied or make any representation that the contents will be complete or accurate or up to date. The accuracy of any instructions, formulae and drug doses should be independently verified with primary sources. The publisher shall not be liable for any loss, actions, claims, proceedings, demand or costs or damages whatsoever or howsoever caused arising directly or indirectly in connection with or arising out of the use of this material.

© Taylor and Francis 2007

## Suitable remote sensing method and data for mapping and measuring active crop fields

H. XIE†, Y. Q. TIAN\*‡, J. A. GRANILLO§ and G. R. KELLER¶

†Department of Earth & Environmental Science, University of Texas at San Antonio,  
San Antonio, Texas 78249-0663, USA

‡Department of Environmental, Earth & Ocean Sciences, University of Massachusetts,  
Boston, Massachusetts 02125, USA

§El Paso Water Utilities, 1154 Hawkins Blvd, El Paso, Texas 79925, USA

¶Department of Geological Sciences, University of Texas at El Paso, El Paso, TX 79968,  
USA

(Received 27 September 2005; in final form 16 March 2006)

The objective of the study was to examine suitable remote sensing methods and data for mapping and measuring the acreages of active crop lands in order to improve irrigation management. We compared classification results from a supervised classification method and a method using normalized difference vegetation index (NDVI) with additional pre-classification processing. IKONOS and Landsat Enhanced Thematic Mapper Plus (ETM+) images were tested to see if high spatial resolution remote sensing data would have significant advantages in distinguishing between active and fallow lands. The classification achieved an overall accuracy of 93.63%. The results showed that the supervised classification did not have a clear advantage over the simple method using NDVI at the level of distinguishing between active crops and fallow lands. The result suggests that using ETM+ instead of IKONOS high spatial resolution imageries is appropriate because of the high cost of IKONOS imageries and image heterogeneity of agricultural fields. It was shown that pre-processing with a mask to exclude the non-agricultural objects blended with agricultural fields is critical.

### 1. Introduction

Knowing the acreage of active crops in a particular irrigation rotation is one of the most important factors for water planning and management, especially for semi-arid and arid environments where water is limited. Efficiency of managing irrigation water is an important issue in arid and semi-arid areas, such as along the Rio Grande Valley area in the south-west USA where there is a major agriculture corridor for the region. The water requirement for an agricultural irrigation rotation usually depends on the area of active crops. Traditionally, water planning for agricultural water uses is conducted by referring to information on the acreage of irrigated agriculture and water supplied in the previous year. Previous water use information is usually incomplete since it consists of volunteer-based reporting from farmers at the end of the year. Also, water demand for agricultural uses can vary

---

\*Corresponding author. Email: [yong.tian@umb.edu](mailto:yong.tian@umb.edu)

significantly from year to year due to the changes of the acreage of active crops. Therefore, mapping and measuring active crops and fallow lands from satellite imagery would be appropriate for agricultural water-use planning.

Using satellite remote sensing technology for mapping irrigated areas was attempted several decades ago (Heller and Johnson 1979, Hoffman 1979, Tinney *et al.* 1979, Thiruvengadachari 1981). In the present decade, there have been new research efforts incorporating the rapid advancement of technology to improve the capability of monitoring agricultural and hydrological conditions of the land surface (Ambast *et al.* 2002). For example, Thome *et al.* (1988) used Landsat Multispectral Scanner (MSS) data and estimated the total irrigated area in the Mendoza province of Argentina. Azzali and Menenti (1996) used temporal data to distinguish the irrigated and non-irrigated crops. Several studies (Vidal and Baqri 1995, Herrero and Casterad 1999) reported the results of using Landsat Thematic Mapper (TM) data to detect irrigated areas or to assess net water requirements in crop fields using supervised classification. A common deficiency of the previous methods of assessing acreages of croplands using remote sensing data is the complexity that is impractical for management purpose. Their classification methods of using regression or supervised training depend on absolute image values so the calibrated coefficients are not transferable to a variety of spatial and temporal conditions. Based on the literature, we question if these complex methods are significant in terms of achieving the required accuracy of classifying between active and fallow lands. One possible solution for simplifying the classification process might be the use of a simple classification method jointly with a pre-processing scheme.

In this study, we examined two land-use classification methods with Landsat Enhanced Thematic Mapper Plus (ETM+) imagery for mapping and measuring the acreages of active crop lands. One is a complex supervised classification method, namely the spectral angle mapper (SAM), which is based on similarity of spectral characteristics of classes to training site (class). The other one is a simple classification method using the normalized difference vegetation index (NDVI) incorporating a pre-classification processing procedure. By comparing to the complex SAM method, this study can determine if the NDVI-based classification with a pre-processing procedure would be a suitable method for irrigation planning. Suitable results for this application would be classification accuracy, less complexity in processing, and cost-effectiveness for required data. In the pre-classification processing, we explore the usefulness of involving ancillary data. The ancillary data include ortho-planimetric layers and land resources, such as road edge, hydro line, hydro area, parcel base-maps, and irrigation boundary. The ancillary data were used to create a mask for delineating agricultural fields by excluding non-agricultural objects.

Additionally, the IKONOS and Landsat ETM+ images were tested with the SAM classification method to see if high spatial resolution remote sensing data would have significant advantages in distinguishing between active and fallow lands. Using ETM+ instead of IKONOS high spatial resolution imageries can avoid high cost of purchasing imageries. Besides the higher cost, the high resolution imagery might not be appropriate to use for land-use with greater heterogeneity. Accuracy of classification with different methods and imageries were assessed using a confusion matrix based on ground data. The study results would be useful in identifying an accuracy-reliable and cost-effective method of extracting acreages of active crop fields and fallow lands for irrigation management and planning.

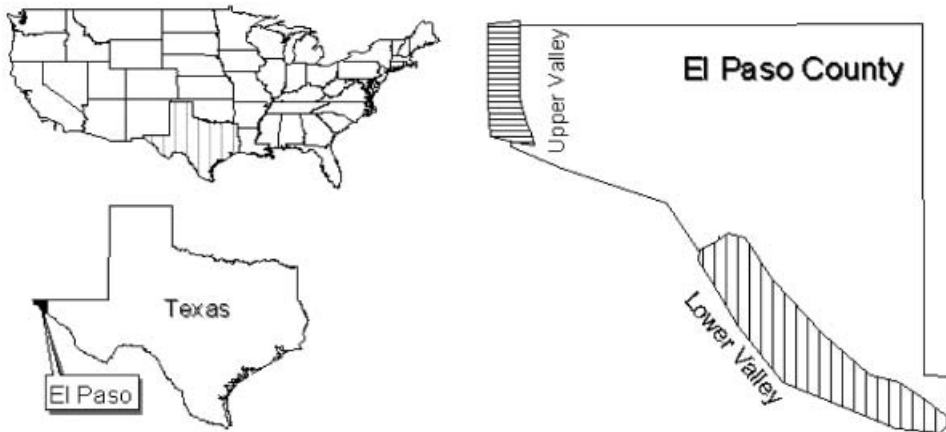


Figure 1. Index map of the study area (El Paso, Texas). The IKONOS images covered two agricultural areas: Upper Valley and Lower Valley.

## 2. Study site and data

The study site is located in El Paso County, Texas, part of the semi-arid area of the south-western USA (figure 1). Agricultural land uses dominate the site, including the Upper Valley and Lower Valley along the Rio Grande River valley. The total irrigated agriculture area is about 47 000 acres. Primary field crop commodities consist of cotton, pecan, corn, wheat, alfalfa, and commercial vegetables.

Two types of imagery data, Landsat ETM+ and IKONOS, were used in the study. Simple dark subtraction method was used for radiometric correction. Five ETM+ images (path 33/row 38) acquired at different times (between 1999 and 2001) were sub-setted to cover the study area (figure 1). Landsat ETM+ has a resolution of 30 m with six multi-spectral bands, one thermal band of 60-m resolution, and one panchromatic band of 15-m resolution. The 386 scenes of IKONOS imagery were acquired by El Paso Water Utilities through a contract awarded to a Californian company. The acquisitions were carried out between August 2000 and February 2001 to satisfy the requirement of cloud free or less than 5% of cloud cover. The images in the Lower Valley portion (south, 251 scenes) acquired from August to October 2000, and in the Upper Valley portion (north, 135 scenes) acquired from August 2000 to February 2001. Each scene is in 1-m spatial resolution (4-m multi-spectral bands fused with 1-m panchromatic band) with four bands: blue (band 1), green (band 2), red (band 3) and near-infrared (band 4). Each image (tile) size is  $1500 \times 1500$  pixels (i.e.  $2.25 \text{ km}^2$ ).

All IKONOS and ETM+ images were geo-referenced against the El Paso street centreline or El Paso Water Utility's (EPWU) digital orthorectified airphotos, which are in 1-foot spatial resolution and acquired in 1997. Both the street centreline and the orthophotos are in Texas central state plane coordinates with North American Datum of 1983 (NAD83).

## 3. Ground investigation (ground data) and analysis

In order to understand the signatures of crops and fallow lands in the images, an area of 2295.7 acres was selected for ground investigation (ground data). The area is covered with four scenes of IKONOS images as displayed in figure 2. Three ground

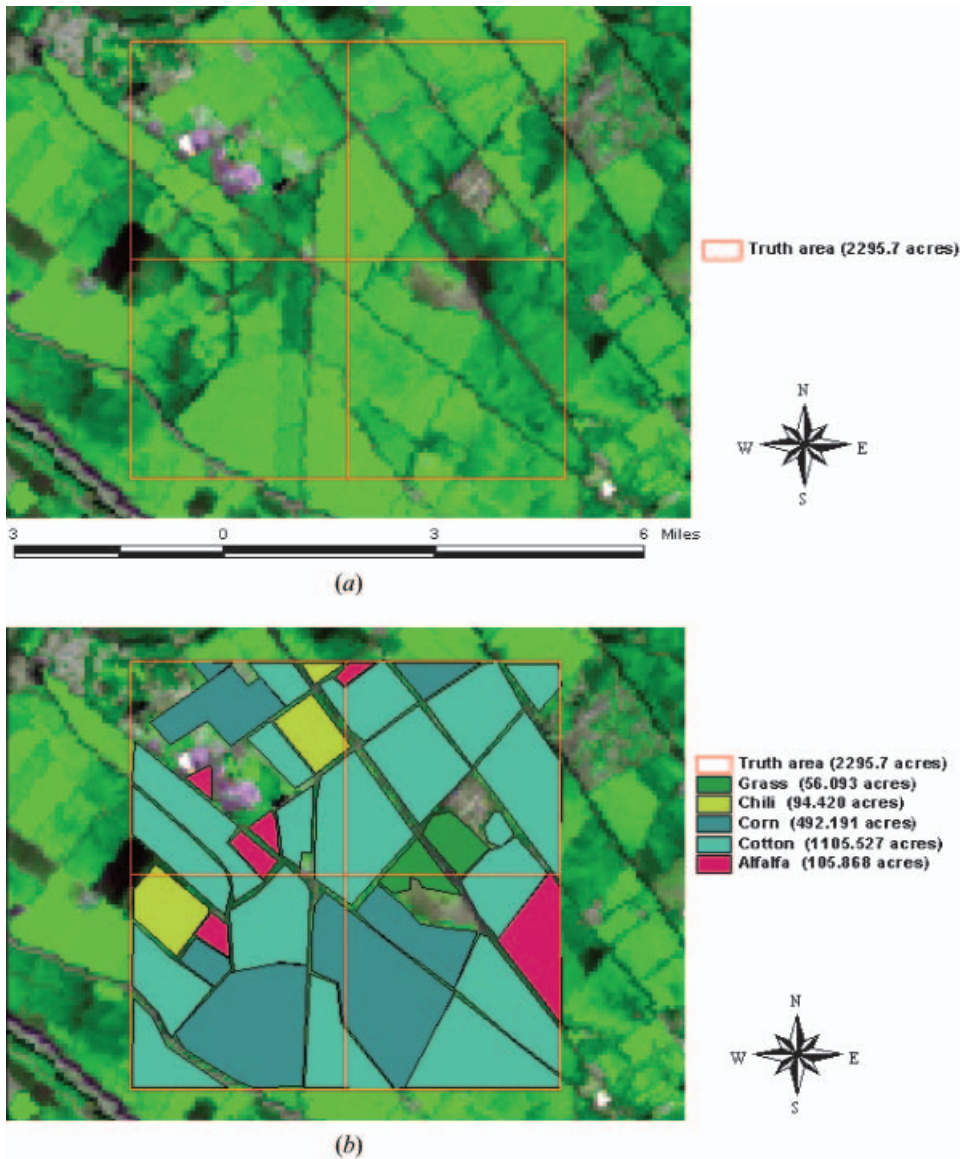


Figure 2. Images and related ground investigation (ground data) results. (a) The ETM+ image of 15 July 2001. (b) The first field data results on 25 July 2002. (c) The IKONOS image of 2000. (d) The interpreted results of (c) by comparison with (a), (b) and the ETM+ image acquired on 7 September 2000 (not shown).

investigations were conducted on 25 July, 18 September, and 6 November 2001, respectively. The ground investigation served for both training and accuracy assessment. The first field investigation in 25 July (figure 2(b)) reflected all agricultural lands in the crop-growing season and no fallow land in the ground data area. The area of crops was about 1854 acres out of the total area of 2295.7 acres (table 1). The remaining areas are residential, school and irrigation ditches. Cotton was the dominant crop ( $\sim 60\%$ ), with corn the second-most dominant crop

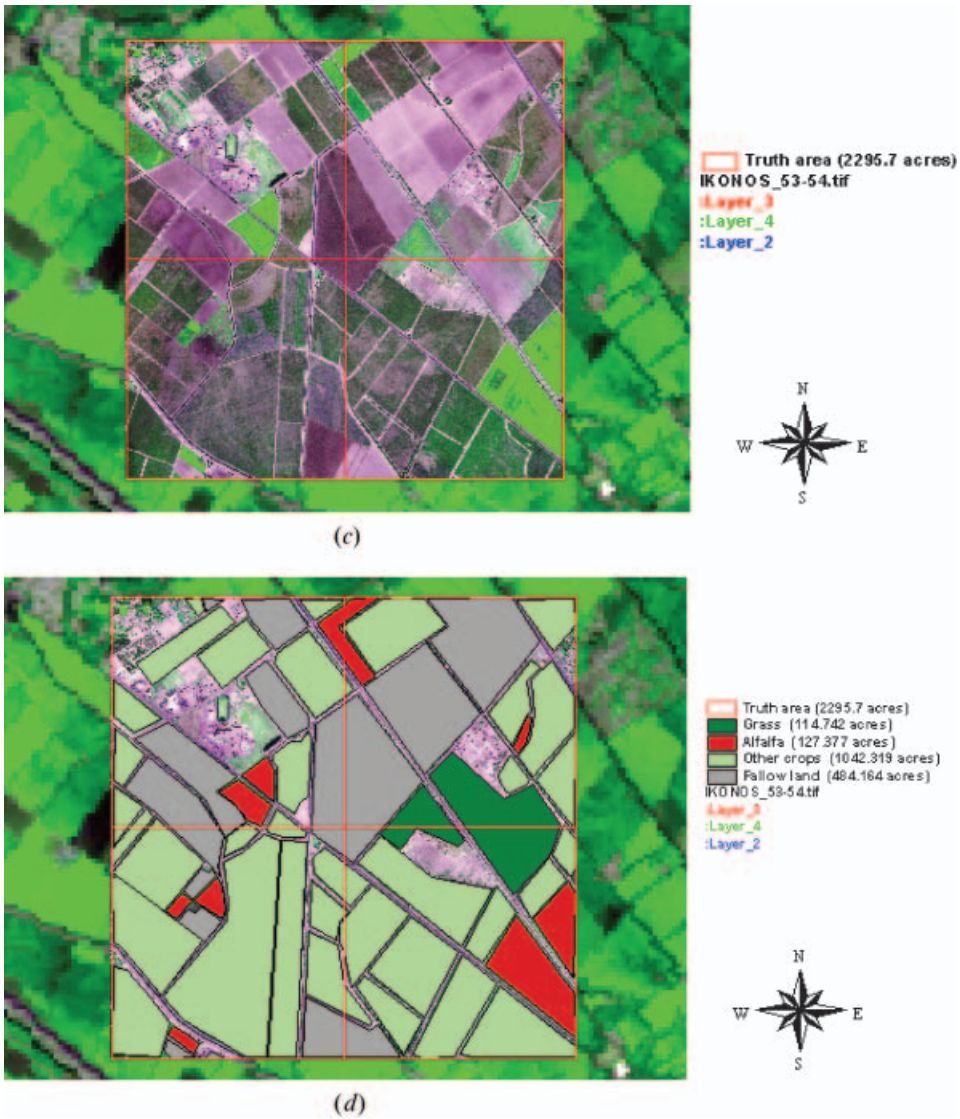


Figure 2. (Continued.)

Table 1. Ground data results (in acres) of July 2001 and interpreted results from IKONOS imagery of 2000. This portion of IKONOS images were acquired in August to October 2000.

	ETM+, 15 July 2001	IKONOS, Aug. to Oct., 2000
Grass	56.093	114.742
Alfalfa	105.868	127.377
Corn	492.191	
Cotton	1105.527	
Chile	94.420	
Other crops		1042.319
Fallow land		484.164
Total	1854.099	1768.602

(~27%). Besides crop lands, fallow lands (the harvested cornfields) were found in the second field investigation carried out on 18 September. This is similar to the situation in the previous year (2000) mapped by IKONOS images, as displayed in figure 2(c). This portion of IKONOS images was acquired mostly in September 2000, although the image acquisitions spanned from August to October 2000. The interpreted results of figure 2(c), combined with information observed from the second field investigation as well as the information from figure 2(a) and (b) are shown in figure 2(d). The acreage of each crop is also included in table 1. The total acreage of the fallow lands in this time of 2000 (mostly September) was 484.164 acres, which is similar to the total acreage of cornfields (492.191) in 2001. Also included from the IKONOS images of 2000 is the 1042.319 acres covered by 'other crops' (table 1). The type of 'other crops' in 2000 is cotton, since cotton is usually harvested later than corn. In the third ground investigation of early November, only cotton (ready to be harvested) and alfalfa remained, while most of the harvested cornfields were growing sorghum, which will be ploughed for soil fertilizer in December.

Overall, the three field investigations provided the baseline information for various crops and experiences for selecting the training sites and for image interpretations.

#### 4. Pre-processing and classifications

##### 4.1 *Excluding non-agricultural fields*

A pre-classification process was conducted to improve classification accuracy. The pre-processing involves the creation of a mask for excluding non-agricultural areas before the classification. Figure 3 is a part of the Lower Valley image mosaicked from 183 IKONOS images. It visually shows that non-agricultural fields (residential, commercial, school, road system) are blended with agricultural fields (green and white polygons). Furthermore, the far right portion (east) of the image is the desert area, while the far left portion (west) of the image is the agriculture area in Mexican side (Rio Grande River is the border of the USA and Mexico). Due to the spectral similarities of objects in multi-spectral imagery, a simple threshold-based NDVI classification method as well as supervised-based classification methods without pre-classification processing are not capable of distinguishing the backyard grasses and trees in the residential area from crops. Similarly, spectral resemblance occurs to parking lots, roads, buildings, even desert area and fallow lands. Therefore, it was hypothesized that creating a mask to exclude the non-agricultural fields would improve the classification accuracy.

Ancillary data in GIS format, such as road edge, hydro line, hydro area, parcel map, and irrigation boundary, were used for the creation of the mask. Road edge covers all of the paved roads (not including the small roads among agriculture fields). Hydro line refers to the small irrigation ditches and hydro area refers to the larger irrigation ditches. Both these two features overlap with most of unpaved roads, although they are much narrower than unpaved roads. Therefore, buffer zones of 25 feet on both sides of the hydro line and hydro area were created to mask these unpaved roads. Parcel maps were used to mask out residential, business, and school areas such as grassy lawns, sports fields, parking lots, and buildings. The irrigation boundary is used to exclude the areas outside the El Paso irrigation area such as the desert area to the east and the Mexican side to the west. Then these five



Figure 3. Portion of the mosaicked IKONOS image (tile rows 42–55) in the Lower Valley. Green and white polygons within the El Paso irrigation area overlaid on the image are the classified agricultural fields. They are active crops and fallow lands, respectively.

types of GIS layers were merged into one shapefile for exclusion from classification. With this shapefile, a mask shapefile that only covers the agriculture fields can then be created. In order to incorporate the mask into classification in ENVI software, a binary image of the mask was first produced from the mask shapefile.

#### 4.2 Supervised classification

There are many supervised classification methods such as parallelepiped, maximum likelihood, Mahalanobis distance, neural network, and spectral angle mapper. For an accurate classification in our preliminary test, we chose the SAM supervised classification in this study. Following usual procedures, we also conducted post-classification with the popular methods, such as combining classes, sieve classes, and clump classes. For simplicity, we only detail the SAM method and the selection of training sites, while all methods and procedures used are summarized in table 2.

**4.2.1 *N*-dimensional visualizer and spectral endmembers selection.** Due to the heterogeneity of the land uses in the study site, training areas (polygons) were carefully handpicked as polygons in GIS throughout the entire irrigation area (not limited in the field data area). Since the same crop type (such as corn) may vary in spectral characteristics from field to field depending on growing status, water stress,

Table 2. Summary of SAM-based classification procedure.

Images	Time	Active crops	Fallow land	
IKONOS	Aug. 2000 to Feb. 2001	SAM threshold: 0.03	SAM threshold: 0.03	
		Combine	Combine	
		Sieve threshold: 4	Sieve threshold: 2	
		Clump operator: $6 \times 6$	Clump operator: $10 \times 10$	
		Sieve threshold: 400	Sieve threshold: 200	
		Clump operator: $9 \times 9$	Class to vector	
		Class to vector		
ETM+	15 Jul. 2001	SAM threshold: 0.10	SAM threshold: 0.05	
		Combine	Combine	
		Sieve threshold: 3	Sieve threshold: 3	
			Class to vector	Class to vector
	26 Apr. 2001	SAM threshold: 0.08	SAM threshold: 0.06	
		Combine	Combine	
		Sieve threshold: 6	Sieve threshold: 10	
		Clump operator: $2 \times 2$	Class to vector	
			Sieve threshold: 10	
			Class to vector	
	7 Sept. 2000	SAM threshold: 0.13	SAM threshold: 0.05	
		Combine	Combine	
Sieve threshold: 50		Sieve threshold: 50		
		Class to vector	Class to vector	
10 Jun. 2000	SAM threshold: 0.13	SAM threshold: 0.05		
	Combine	Combine		
	Sieve threshold: 10	Sieve threshold: 10		
		Class to vector	Class to vector	
12 Sept. 1999*	SAM threshold: 0.35	SAM threshold: 0.20		
	Combine	Combine		
	Sieve threshold: 10	Sieve threshold: 25		
		Class to vector	Class to vector	

\*SAM threshold values in this image are larger than others (see explanation in §4.2.2).

pest infestation, and soil type, we usually picked many sites of each variation and then grouped all of them into one crop (corn, for example). Similarly, we also grouped many sites of bare soils, harvested lands, or ploughed fields throughout the entire irrigation area as fallow lands. The field investigations (§3) significantly helped the selection of training sites for July 2001. For other old images—four scenes of ETM+ images and all IKONOS images—the selection of training sites completely depended on expert's knowledge due to the project not beginning until June 2001. The training polygons selected in GIS were converted as regions of interest (ROIs) in ENVI (image processing software). These ROIs were used in the *N-dimensional visualizer* of ENVI to identify the purest pixels (i.e. most extreme spectral responses), or spectral endmembers.

**4.2.2 SAM classifier.** The SAM classifier is a physically-based spectral classification method that uses *n*-dimensional angles to match pixels to reference spectra. The algorithm determines the similarity between two spectra by calculating the angle between the spectra, treating them as vectors in a space with dimensionality equal to the number of bands. This technique, when used on calibrated reflectance data, is relatively insensitive to illumination and albedo effects. The SAM classification was

conducted for both ETM+ and IKONOS images to classify the active crops and fallow lands of the El Paso County.

An endmember spectrum used by SAM in this study was first extracted directly from the ROIs by averaging spectra derived from the previous section. SAM compares the angle between the endmember spectrum vector (ROI) and each pixel vector of the image in  $n$ -dimensional space. Smaller angles (in radians) represent closer matches to the reference spectrum. Pixels with a spectral angle larger than a user-specified maximum angle threshold (in radians) are not classified (*ENVI User's Guide*, Research System, Inc. 2000, Kruse *et al.* 1993). Selecting the maximum angle threshold value is an important factor for successfully using SAM classification. Crosta *et al.* (1998) noticed that changes in the value of the threshold produced significant changes in the number of pixels classified as one of the reference spectrum. For that reason, we tested numerous threshold values for each case, and selected a value that resulted in the best classification compared with field data or conceptual valuation based on experiences.

For the IKONOS images, the threshold value of 0.03 is the best value for both active crops and fallow land (table 2). For ETM+ images, the best values are 0.08–0.13 for active crops, and 0.05–0.06 for fallow land except for the ETM+ image of 12 September 1999. The endmembers of the 1999 image came directly from the image of 7 September 2000 due to being the same time of year. However, these endmembers worked very well for the year 2000 images, but did not work well for the 1999 image. As a complement, endmembers for the image of 1999 were readjusted by adding new endmembers and deleting some existing ones, and the threshold values were increased to be much larger than the previous threshold values used for the image of year 2000 (table 2). This experience suggests that (1) the training endmembers usually vary greatly for multi-temporal images, even for the two images acquired in almost the same day (or month) in different years; and (2) there are limitations for any standard spectral library due to varying atmospheric and illumination conditions since perfect atmospheric correction is impossible. Table 2 summarizes the key processes in the classification. Figure 4 is the general work flow chart of SAM-based classification procedure for using an ETM+ image. The non-agricultural fields were all excluded from IKONOS and ETM+ images by using the mask created in §4.1.

### 4.3 NDVI-based classification

Vegetation indices have been widely used for tracking green biomass, leaf area index of crop canopies, and fractional amount of net radiation (Hatfield *et al.* 1984; Daughtry *et al.* 1990, Jackson and Huete 1991, Kustas *et al.* 1993). NDVI is one of the most widely used indices for indicating the amount of green vegetation present in a pixel—higher NDVI values indicate more green vegetation (Jensen 1986, Jackson *et al.* 1988; Pinter *et al.* 2003). The NDVI method transforms multi-spectral data (bands 3 and 4 of ETM+) into a single image representing the vegetation distribution by using equation (1):

$$\text{NDVI} = \frac{b_4 - b_3}{b_4 + b_3} \quad (1)$$

where  $b_3$  and  $b_4$  are band 3 and band 4 of the ETM+ image, respectively. Valid results fall between  $-1$  and  $+1$ . The larger the pixel value, the higher the fraction of vegetation cover within the pixel. After using the relative atmospheric correction

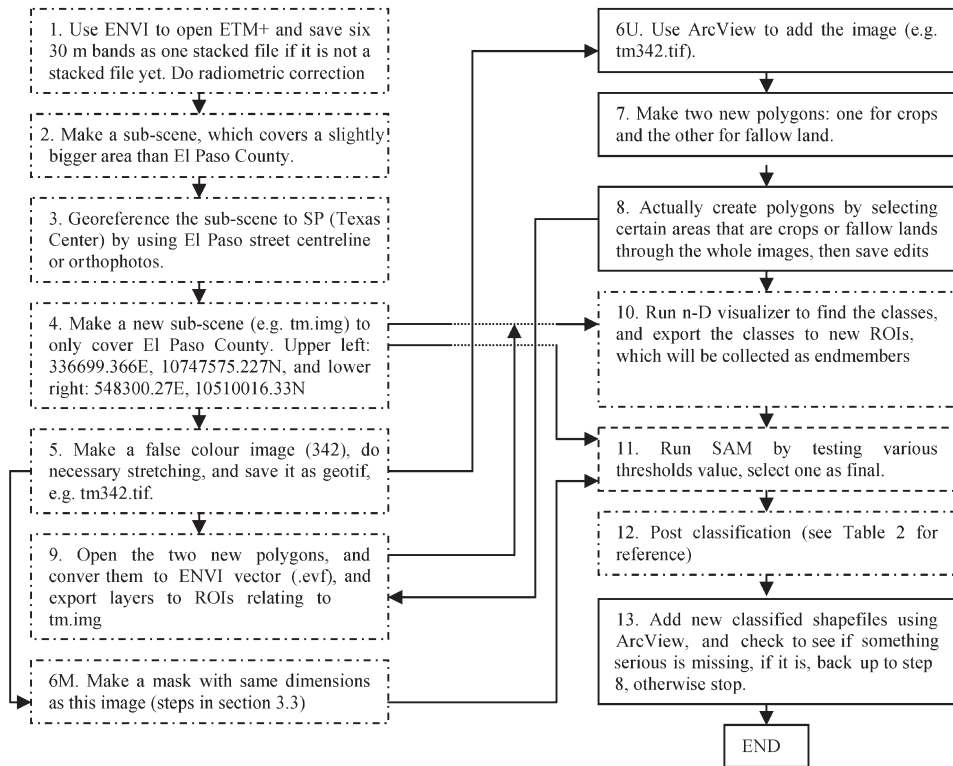


Figure 4. SAM-based classification procedure using integrated remote sensing-GIS technology. Steps with dashed-line frames are remote sensing methods, and steps with solid-line frames are GIS methods.

(dark subtraction) method, many threshold values were examined against ground data. A threshold NDVI of 0.15 was found to produce the highest classification accuracy for separating vegetation cover from other land covers.

The work flow chart in figure 5 describes the NDVI-based classification scheme with GIS (ArcGIS) and remote sensing software (ENVI). The process with the NDVI-based method as described in this flowchart is more time efficient than the one with the SAM method (figure 4). Using the SAM method is time consuming since the selection for training sites is labour intensive and depends on professional experiences. The NDVI method is efficient since it does not require training site selection. It is also computation efficient (several hours for classifying one image compared with 2–3 days with the SAM method since selecting the training site is labour intensive and needs professional experience).

## 5. Classification results and accuracy assessment

The results produced from both supervised (SAM) and NDVI-based classification approaches on multi-temporal ETM+ images covering a period of 3 years (29 September 1999, 10 June 2000, 7 September 2000, 26 April 2001, and 15 July 2001) are illustrated in tables 3 and 4, respectively. Since one scene of ETM+ image covers the entire county's agriculture area, the classification result should reflect the actual situation in an irrigation rotation.

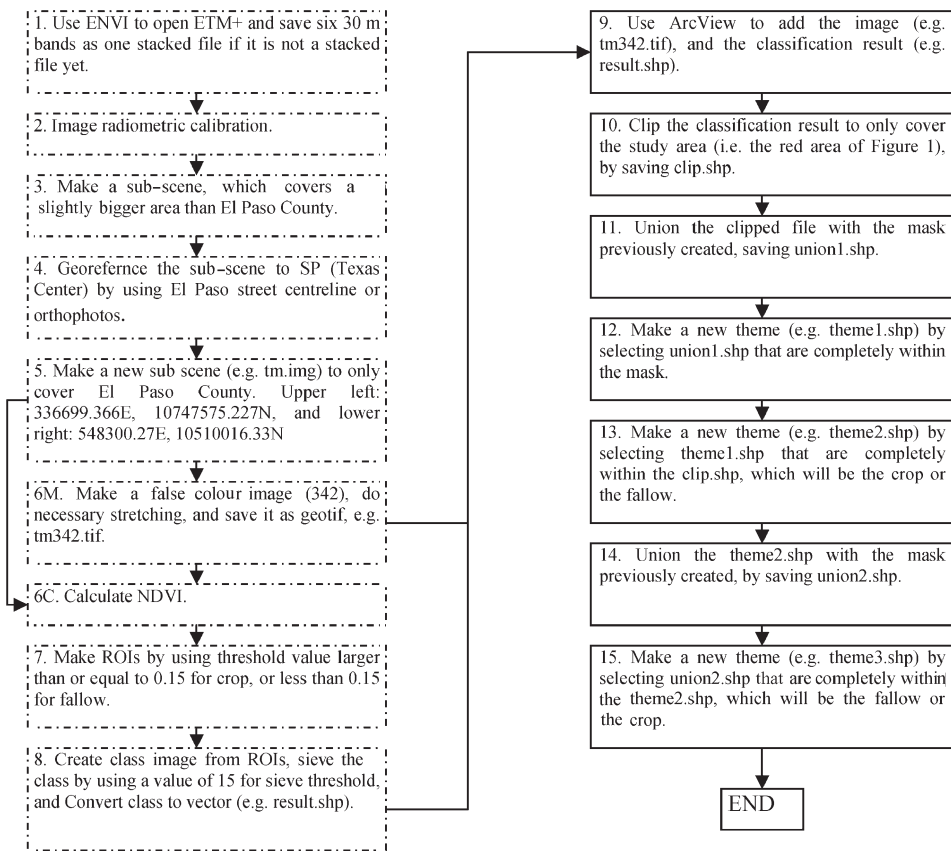


Figure 5. NDVI-based classification procedure using integrated remote sensing–GIS technology. Steps 1–8 (dashed-line frames) are remote sensing methods, and steps 9–15 (solid-line frames) are GIS methods.

The classification using the SAM method resulted in 42 374 acres of active crops and 4826 acres of fallow lands for the ETM+ image of 15 July 2001 (table 3). The confusion matrix and ground data information were employed to assess the accuracy of the classifications. This was the only adopted imagery whose acquisition time matched the first of the three field data. Figure 6(a) shows the ground investigation on the image of 15 July 2001 (field data on 25 July), and figure 6(a) is the SAM classification result. The number of total pixels in the ground data was 8495 (figure 6(a)). All of the pixels are crop lands; there were no fallow land during

Table 3. Classification results from SAM-based procedure.

		Crops (acres)	Fallow (acres)
IKONOS ETM+	Aug. 2000–Feb. 2001	35 319	11 881
	15 Jul. 2001	42 374	4826
	26 Apr. 2001	16 030	31 170
	07 Sep. 2000	39 656	7544
	10 Jun. 2000	35 592	11 608
	12 Sep. 1999	41 764	5436

Table 4. Classification results from NDVI-based procedure.

Images and date	Crops (acres)	Fallow (acres)
ETM+ 15 Jul. 2001	42 168	5032
26 Apr. 2001	14 163	33 037
07 Sep. 2000	38 358	8842
10 Jun. 2000	38 203	8997
12 Sep. 1999	42 451	4749

this time (figure 2(a) and (b)). Of these, 7954 were correctly classified as crop lands in figure 6(b). The accuracy is 93.63%, and unclassified is 6.37%.

Using the NDVI classification method (table 4) for the same image acquired in 15 July 2001, 42 168 acres of active crops and 5032 acres of fallow lands were classified. The results from NDVI differencing matched well to the results of SAM classification (with 93.63% overall accuracy). Figure 7 shows the comparison of classification results of crop lands and their percentage differences based on SAM and NDVI from the five images. The percentage difference is calculated by the equation:

$$\text{difference}(\%) = \frac{\text{acres}_{\text{NDVI}} - \text{acres}_{\text{SAM}}}{\text{acres}_{\text{SAM}}} \times 100 \quad (2)$$

where  $\text{acres}_{\text{NDVI}}$  and  $\text{acres}_{\text{SAM}}$  are acres of active crops classified using the NDVI and SAM methods, respectively. From the figure, it is clear that by using the SAM and NDVI methods, the classification accuracies are almost the same. The percentage of differences between two methods are from the minimum of  $\sim 0\%$  for the image for 15 July 2001 to the maximum of  $\sim 12\%$  for the image for 26 April 2001. Similar accuracy suggests that the more complex supervised SAM method did

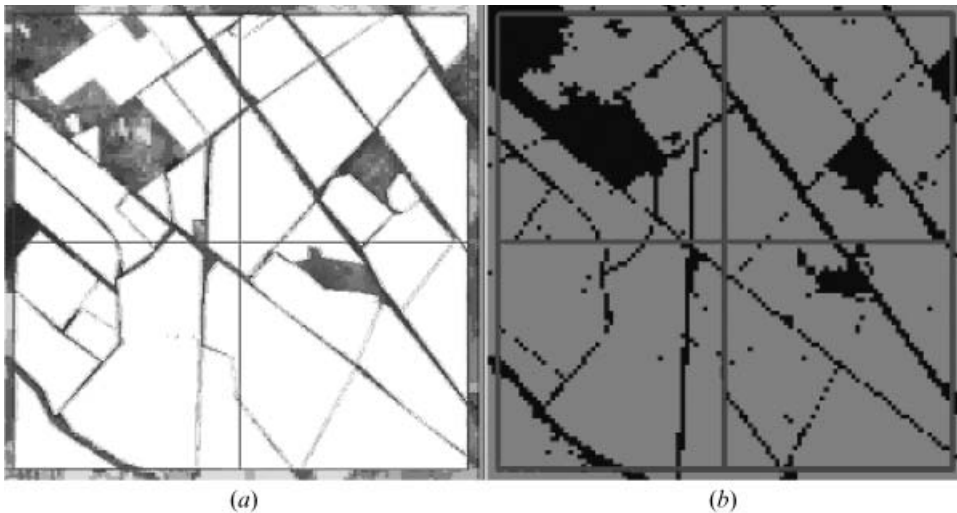


Figure 6. The ground data (a) and classification result (b) of the ETM+ image on 15 July 2001. (a) Ground data result, with white as crops (see figure 2(b)); (b) is the classification result, with light grey as crops.

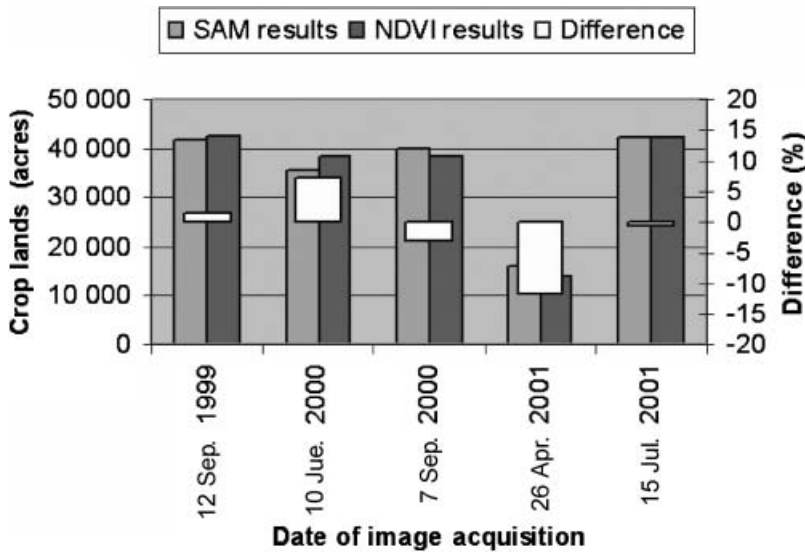


Figure 7. Comparison of classification results of crop lands from SAM and NDVI and their differences in percentages.

not show significant advantage over the NDVI differencing. In other words, the NDVI method jointly with a pre-classification processing is sufficient for separating between active crops and fallow lands. In addition to accuracy assessment, the NDVI method requires only threshold values for transformation from NDVI to ROIs and a process of excluding non-agricultural fields blended with agricultural areas. Therefore, the NDVI method is more straightforward to use compared to the SAM method.

The differences between SAM and NDVI method are (1) SAM uses all available spectral bands such as six bands for the ETM+ image and four bands for the IKONOS image, while NDVI uses only two bands (bands 3 and 4 for both ETM+ and IKONOS); and (2) SAM is a supervised classification method, requiring selection of training sites before classification, while NDVI does not. SAM is very good for a hyperspectral image (spectral resolution 20 nm or better) where hundreds of spectral bands (wavelengths) are used for classification, while NDVI only uses two spectral bands or wavelengths (red and near-infrared), which does not represent the whole spectral picture of an object. For a multi-spectral image (spectral resolution 200 nm or worse), however, only six or four bands are available. So it does not make too much difference whether the SAM or NDVI method is used, however the SAM method is complex in three aspects:

- (1) It requires ground investigation for selection of training sites, which is not always possible or convenient. For example, it is impossible to conduct ground investigation for images acquired in past years. So selecting training areas when using old images depends completely on the experience of an interpreter. This is the case of this study: four ETM+ images (before 15 July 2001) and all IKONOS images.
- (2) Collection of endmembers with the  $N$ -dimensional visualizer in ENVI is an interactive tool depending largely on the knowledge of experts.

- (3) The threshold value (the maximum angle) in the SAM method is very sensitive to the classification results. The threshold value selection requires exhaustive searching and the experience of an interpreter.

On the other hand, the NDVI method does not have above deficiencies for the purpose of classifying crop lands from fallow lands, and will perform the same for any image no matter whether current or old, because NDVI does not involve the selection of training sites and it does not require a very experienced interpreter. So NDVI could provide better, reliable, and consistent accuracy of classification results for the purpose of water management.

Having carried out the above analysis, we should point out that the supervised SAM classification is adequate for classifying different crops such as cotton, corn, and alfalfa if proper spectral resolution imagery is used. However in this case, all these different crops will be grouped into one class: active crops. The remaining objects are in fallow land. In other words, these two classes are either green or non-green, which was accurately separated by the NDVI method. However, without the mask previously built, it is difficult to achieve high accuracy of classification from both NDVI and SAM methods based on the ETM+ imagery.

The results of using SAM classification on the entire mosaicked IKONOS image did not match the real situation very well, because 386 scenes of IKONOS images were acquired, spanning a time period of different irrigation rotations (August 2000 to February 2001).

As an example, figure 8 shows the classification result by using the SAM method on IKONOS images. It was visually observed that crops in a field are not homogeneous (figure 8(a)). The SAM classification (figure 8(b)) overlaying on the IKONOS image could identify bare areas (patches) inside agricultural fields. These holes (patches) represent that these crops are in poor condition: less water, less fertility, more pests, or salt accumulation. Miyamoto (2000) concluded that most of these holes are due to salt accumulation, because the soil in these fields is silt clay, which has features such as inadequate soil permeability and lower water infiltration, especially when the soil is compacted or affected by sodium. The information is very useful in farming management such as watering, fertilizing, identifying presence of pests, or assessing water quality. In other words, it is useful to achieve precision agriculture. A disadvantage is that these holes could cause mis-classification between a crop land in poor conditions and a fallow land. This suggests that the higher resolution of IKONOS imagery does not guarantee higher classification accuracy in this case. The results based on ETM+ imagery may ignore these holes and obtain better classification results except for those holes bigger than 30 m.

## 6. Conclusions

This study evaluated a NDVI differencing method combined with pre-processing to exclude non-agricultural fields for mapping and measuring the acreages of active crop lands in order to improve irrigation management. The evaluation was based on Landsat ETM+ images and was through the comparison to a supervised classification method, namely SAM. The similar classification accuracies from the two methods demonstrated that the more advanced classification, the SAM approach, did not have a clear advantage compared to the method using NDVI at the level of distinguishing between active crops and fallow lands, except its potential to make more detailed classification, such as further classifying crops into corn,



(a)



(b)

Figure 8. Classification catches these holes (bare areas) inside fields. (a) The IKONOS image and (b) the classification results overlaying the image.

cotton and alfalfa. However, this potential capability of the SAM method came with the more complex processing (such as selection of training sites,  $N$ -dimensional visualizer, selection of spectral endmembers, and post-classification) and exhaustive searching for some proper threshold values (such as specifying the spectral angle threshold and sieve pixel threshold). The accurate classification from the relatively simple method of using NDVI differencing demonstrated that involving ancillary data in pre-classification processing is an effective scheme for avoiding a complex classification method. Because it is accuracy-reliable and cost-effective, we

recommend the NDVI method with pre-processing to exclude some of the unwanted objects as a practical approach in mapping and measuring the acreage of active croplands for irrigation management and planning.

A comparative test was also made to see if high spatial resolution remote sensing images would have significant advantages in extracting active crop lands from an agricultural region. By examining IKONOS and Landsat ETM+ images, it is clear that using ETM+ instead of IKONOS high spatial resolution imageries is appropriate in this application. When using high resolution images it is difficult to handle the heterogeneity of agricultural fields, so salt and pepper effects are unavoidable (Yu *et al.* 2006), such as wrong classification patches caused by water stress, by presence of pests, or by accumulation of salt. This result made this testing worthwhile, because using ETM+ would also have the advantage of avoiding the high cost of purchasing IKONOS images and would be an appropriate data source for irrigation management in arid or semi-arid areas. The study provided valuable insights into selecting an appropriate classification method as well as a proper type of imagery for increasing classification accuracy, reducing complexity, enhancing computation efficiency, and maximizing the cost efficiency.

### Acknowledgements

This project was funded by the El Paso Water Utilities (EPWU). Special thanks are extended to Armando Renteria, manager of the Department of Information System, Nick Costanzo, chief financial officer, and Ed Archuleta, general manager of the EPWU. A portion of this work was also supported under cooperative agreement NCC5-209 (PACES) at the University of Texas at El Paso. The authors would like to thank two anonymous reviewers for their helpful comments that improved the paper.

### References

- AMBAST, S.K., KESHARI, A.K. and GOSAIN, A.K., 2002, Satellite remote sensing to support management of irrigation systems: concepts and approaches 1. *Irrigation and Drainage*, **51**, pp. 25–39.
- AZZALI, S. and MENENTI, M., 1996, Fourier analysis of temporal NDVI in the southern African and American Continents. Report 108, DLO-Winand Staring Centre, Wageningen, The Netherlands.
- CROSTA, A.P., SABINE, C. and TARANIK, J.V., 1998, Hydrothermal alteration mapping at Bodie, California, using AVIRIS hyperspectral data. *Remote Sensing of Environment*, **65**, pp. 309–319.
- DAUGHTRY, C.S.T., KUSTAS, W.P., MORAN, M.S., PINTER, P.J., JACKSON, R.D., NICHOLS, P.W. and GAY, L.W., 1990, Spectral estimates of net-radiation and soil heat-flux. *Remote Sensing of Environment*, **32**, pp. 111–124.
- HATFIELD, J.L., ASRAR, G. and KANEMASU, E.T., 1984, Intercepted photosynthetically active radiation estimated by spectral reflectance. *Remote Sensing of Environment*, **14**, pp. 65–75.
- HELLER, R.C. and JOHNSON, K.A., 1979, Estimating irrigated land acreage from LANDSAT imagery. *Photogrammetric Engineering & Remote Sensing*, **45**, pp. 1379–1386.
- HERRERO, J. and CASTERAD, M.A., 1999, Using satellite and other data to estimate the annual water demand of an irrigation district. *Environmental Monitoring and Assessment*, **55**, pp. 305–317.
- HOFFMAN, R.O., 1979, Identifying and locating land irrigated by centre pivot irrigation system using satellite imagery. In *Proceedings of Symposium on Identifying Irrigated*

- Lands Using Remote Sensing Techniques – State of the Art*, Missouri River Basin Commission and USGS, Eros Data Centre: South Dakota, USA.
- JACKSON, R.D. and HUETE, A.R., 1991, Interpreting vegetation indexes. *Preventive Veterinary Medicine*, **11**, pp. 185–200.
- JACKSON, R.D., KUSTAS, W.P. and CHOUDHURY, B.J., 1988, A re-examination of the crop water-stress index. *Irrigation Science*, **9**, pp. 309–317.
- JENSEN, J.R., 1986, *Introductory Digital Image Processing* (Englewood Cliffs, NJ: Prentice Hall).
- KRUSE, F.A., LEFKOFF, A.B., BOARDMAN, J.B., HEIDEBRECHT, K.B., SHAPIRO, A.T., BARLOON, P.J. and GOETZ, A.F.H., 1993, The spectral image processing system (SIPS)—interactive visualization and analysis of imaging spectrometer data. *Remote Sensing of Environment*, **44**, pp. 145–163.
- KUSTAS, W.P., DAUGHTRY, C.S.T. and VANOEVELEN, P.J., 1993, Analytical treatment of the relationships between soil heat-flux net radiation ratio and vegetation indexes. *Remote Sensing of Environment*, **46**, pp. 319–330.
- MIYAMOTO, S., 2000, Soil resources of El Paso, characteristics, distribution, and management guidelines, Texas A&M University, Agricultural Research Center at El Paso, US Bureau of Reclamation under grant No. 1425-97FC-40-21650.
- PINTER, J.P., HATFIELD, J.L., SCHEPERS, J.S., BAENES, E.M., MORAN, M.S., DAUGHTY, C. and UPCHURCH, D.R., 2003, Remote sensing for crop management. *Photogrammetric Engineering and Remote Sensing*, **69**, pp. 647–664.
- RESEARCH SYSTEM INC., 2000, *ENVI User's Guide, 2000*, Research System, Inc.
- THIRUVENGADACHARI, S., 1981, Satellite sensing of irrigation patterns in semi-arid areas - an Indian study. *Photogrammetric Engineering and Remote Sensing*, **47**, pp. 1493–1499.
- THOME, R., YANEZ, H.E. and ZULUAGA, J.M., 1988, Determinacion del area bajo riego en la provincia de Mendoza. In *Mechanismos de aprovechamiento hidrico en la region Andina: Imagenes satelitarias y modelos de simulacion*, M. Menenti (Ed.) (Mendoza, Argentina: Instituto Nacional de Ciencia y Tecnicas Hidricas), pp. 203–227.
- TINNEY, L., WALL, S., COLWELL, R. and ESTES, J., 1979, Application of remote sensing for California irrigated lands assessment. In *Satellite Hydrology*, M. Deutsch, D.R. Wiesnet and A. Rango (Eds). American Water Resources Association, **44**, pp. 1421–1426.
- VIDAL, A. and BAQRI, A., 1995, Management of large irrigation projects in Morocco. In *Use of Remote Sensing Techniques in Irrigation and Drainage*, Water Reports 4, A. Vidal, and J.A. Sagardoy (Eds) (Rome: FAO), pp. 99–105.
- YU, Q., GONG, P., CLINTON, N., KELLY, M. and SCHIROKAUER, D., 2006, Object-based detailed vegetation classification with airborne high spatial resolution remote sensing imagery. *Photogrammetric Engineering and Remote Sensing*, **72**, pp. 799–811.